Experimental Analysis of Solar Dish Concentrators with Cylindrical, Oval, and Conical Cavity Receivers

Zainab I. Abdulrazzaq ALhsani *, Ra'ad K. Mohammed Al dulaimi *‡

* Department of Mechanical Engineering, Al-Nahrain University, Baghdad 64074, Iraq

(zynab.isaam1986@gmail.com, dr.raadaldulaimi@eng.nahrainuniv.edu.iq; eng.raadalduleimi@gmail.com)

‡ Ra'ad K. Mohammed Al dulaimi, Tel: +964 7730330677,

Abstract-Three experimental models including cylindrical, oval, and conical cavity receivers were analyzed and tested to estimate the optimum geometry for parabolic dish collector cavity receivers PDC_{cr}. The main contribution of this paper is that new experimental models are suggested and examined to strengthen the capability of absorbers of solar thermal dish collectors to absorb solar energy. The models were examined for three values of mass flow rates and five values of inlet temperatures of the heat transfer fluid. The thermal performance was evaluated by estimating the thermal efficiency η_{th}, exergetic performance η_{ex}, and pressure difference. The results recorded the highest values of η_{th} and η_{ex} for the conical cavity receivers, equal to (η_{th} =82.1%) and (η_{ex} =23.76%), and the lowest values of the pressure drop.

Keywords Concentrated solar energy, solar thermal dish collector, cavity receivers, spiral, pressure drop, collector efficiency

1. Introduction

Solar energy is a worthwhile source of energy that is essential to the energy scope, like for universal warming and fossil fuel reduction.

Sunshine is the most plentiful provenance of energy on Earth. Yearly, the Sun transmits more than 10,000 times the amount of energy exploited by humans [1, 2].

Concentrating solar systems are typical options to produce great amounts of beneficial thermal energy with convenient performance [3].

Among all concentrated solar power (CSP) technologies, the parabolic dish collector (PDC) technology is seen as most valuable because its high concentration ratios [4] rise the performance of the power cycle. With this great advantage and the recent focus on lessening the price and rising the efficiency of PDCs, many investigators have been motivated to focus on PDC_{cr} engineering, and one of the primary functions that researchers work on is the optimum shape of receivers.

Aldulaimi [5] experimentally suggested and examined a new design composed of a dual-layer, staggered configuration and multiscale diameter pipes. The new model is based on the utilization of the inefficient regions of the solar absorber, that is, surfaces which are weak in transforming solar energy to thermal energy within HTF that consist of the gap between the pipes and the terminal sides of the tubes. Five models of dish collector receivers with various staggered diameter ratios between the two layers were examined. The highest value of thermal efficiency was recorded with a staggered diameter ratio of 0.269.

Thirunavukkarasu V. and Cheralathan M. [6] experimentally examined the energy and exergy efficiency of an external-type spiral tube absorber with three different radiation conditions (750 W/m², 600 W/m² and 380 W/m²) and a temperature range of 30℃ to 100℃ with water as the HTF. The authors noted that beam radiation adds to the various in the temperature of the heat transfer fluid between the outlet and inlet of the absorber, which considerably impacts the absorber output and efficiency values.

Furthermore, they recorded 56.21% and 5.45% for the average thermal and exergy efficiencies, respectively, at a beam radiation rate that equal 750 W/m².

Lan et al. [7] utilized a thorough simulation method combining the Monte Carlo ray-tracing (MCRT) method and the finite volume method (FVM) to simulate the optical and thermal performance of a cylindrical cavity absorber in a PDC by simulating the complex photothermal conversion of the PDC_{cr}. The comprehensive photothermal conversion procedure is divided into receiver walls that absorb solar energy as thermal

energy, where the optical performance is estimated by the MCRT and the solar flux distribution on the walls is defined, and receiver walls that transmit thermal energy to the heat transfer fluid (HTF) and ambient air, where the thermal performance is estimated by the FVM model in which the solar flux on the walls is considered as a source term. This study clarified that the arrangement of absorber position, rim angle, tilt angle and emissivity will raise the photothermal transmutation efficiency by 2.6%, 2.4%, 8% and 1.8%, respectively.

Reyhaneh et al. [8] experimentally studied a cubical cavity absorber utilizing Al_2O_3/oil nanofluid and pure thermal oil. Then, the authors compared the results with an itemized literature review of studies about PDC_{cr} with a view to clarify an overall overview of cavity absorbers (including cylindrical, hemispherical, and cubical cavities) utilizing various nanofluids (involve Al_2O_3/oil, MWCNT/oil, and SiO/oil nanofluids). The outcomes showed that the hemispherical and cubical cavities are the most efficient receivers, while the cylindrical cavity presents weak performance. Furthermore, it was stated that the use of nanofluids always causes thermal performance reinforcement.

Kuldeep A., Mohd K. K. et al. [9] numerically investigated the performance of an inverted conical cavity exposed to constant heat flux at its external surface with its internal surface insulated using ANSYS FLUENT version 17.2, using water as the HTF.

Furthermore, the numerical model was verified by experimental results. The results of the suggested model were also matched with the outcomes of numerical simulation of flow through similar upright conical and cylindrical absorber cavities. The authors showed that for the conical cavity in an inverted position, nearly 27.6% of the average rise in Nu was recorded for the entire range of Re compared to that of the conical cavity in an upright position.

Alireza et al. [10] examined three various models of cavity receivers, involve cylindrical, cubical and hemispherical, as solar dish receivers for solar desalination performance in addition to other different solar dish parameters and various humidification-dehumidification desalination parameters, including the solar working fluid inlet temperature, the water-to-air flow ratio and the water flow rate. The highest freshwater output and minimal gain output ratio were obtained by the hemispherical cavity absorber.

Ovidio et al. [11] analyzed the thermal performance of various absorbers, such as a flat-plate absorber and a cavity absorber (Whether the glass cover is available or not). Furthermore, a detailed investigation covering losses such as radiation, natural and forced convection, and conduction was implemented, and new correlations for natural and forced convection were developed. The outcomes showed a considerable increase in the efficiency of the cavity absorbers compared with the flat-plate absorber with much lower working temperatures.

Evangelos et al. [12] investigated five various cavity receivers (cylindrical, rectangular, spherical, conical and cylindrical-conical) under different operating temperature levels and different geometric parameters (the cavity length, the cone angle and the distance from the collector base). Based on the details reported by studies in the literature and using a developed model in SolidWorks Flow Simulation, the results were proved by the literature empirical data.

Depending on the outcomes, the highest performance occurred with a cylindrical-conical shape, followed by the conical and spherical shapes. The worst shape was rectangular, while the cylindrical shape was the fourth-best model in the showing sequence.

Sara et al. [13] experimentally and theoretically investigated a helical baffled cylindrical cavity receiver. Different geometrical and structural parameters were studied for the thermal performance, such as the absorber aperture distance to the focal point ratio, absorber aspect ratio and system geometrical concentration ratio, as well as experimental parameters like the heat transfer fluid (HTF) inlet temperature, mass flow rate and solar irradiation intensity. The results indicated that the optimal selection of the referenced parameters gives 65% thermal performance.

Loni et al. [14] numerically and experimentally studied two shapes of cubical and cylindrical cavity absorbers. Furthermore, numerical modeling was performed to optimize and estimate the cavity receiver performance. The outcomes clarified that the thermal efficiency of the cubical cavity absorber (which recorded 65.14%) was higher than the thermal efficiency of the cylindrical cavity absorber (which recorded 56.44%) in the steady-state period.

Ahmed et al. [15] examined the optical efficiency and the flux distribution of three various designs of cavity receivers, cylindrical, conical and spherical, with the aim of studying their conduct utilizing a developed ray-tracing method. The conical shape receiver recorded the highest optical and thermal efficiency compared with the other models. The optical efficiency was 75.3%, 70.1% and 71.5% for the conical, spherical and cylindrical shapes, respectively, at a surface absorptivity of 85%. The outcomes of the simulated work were corroborated utilizing empirical work in the literature. Different designs of solar absorbers for PDCs were studied [8, 16] to find the optimal shape which has highest performance.

The main contribution of this study is an experimental investigation of three development shapes of cylindrical, oval, and conical cavity receivers to estimate which shape of receiver receives and absorbs more reflected flux energy than the other shapes under different operation conditions, such as variable mass flow rates of the HTF and variable inlet temperature of the HTF.

2. Experimental System

The details of the experimental system of the solar dish collector are presented in a photograph in Fig. 1 and a sketch in

Fig. 2. The basic geometrical dimensions and specification of the examined system are referred in Table 1.

The main structure of the reflective part of the solar collector was composed of 24 ribs made of 6 mm steel plates that were cut into a parabola curve. Then, the ribs were assembled with five ring ribbons also made of a 6 mm steel plate, composing the final structure of the reflective part. Finally, the samples were wrapped with a highly reflective sheet.

The collector was mounted on an iron structure with a height of 110 cm. To orient the aperture of the concentrator vertically to the Sun continuously from sunrise to sunset, the collector rotates around two axes (the first is around a north-south axis, and the second is around a west-east axis) by two linear actuators, as shown in Figs. 1 and 2.

Three models of cavity receivers were suggested and examined experimentally in this study: cylindrical, oval, and conical cavity receivers.

A TM500 12-Channel data logger was employed to find the temperature of the HTF at the inlet and outlet and the average temperature of the outer surface of the receiver. The measurement of temperatures occurred through 12 thermocouples (K-type): two for the inlet and outlet and ten for the surface temperatures. The differential pressure of the HTF was recorded by a differential pressure manometer (407910). An accurate flowmeter was utilized to measure the mass flow rate of the HTF with an accuracy of $\mp1\%$. To control the temperature input of the HTF, a constant heat flux source (heater) with multiple ranges was used, as shown in Fig. 3. A storage insulated tank with a gauge of 1000 L was used to provide water to the collector.

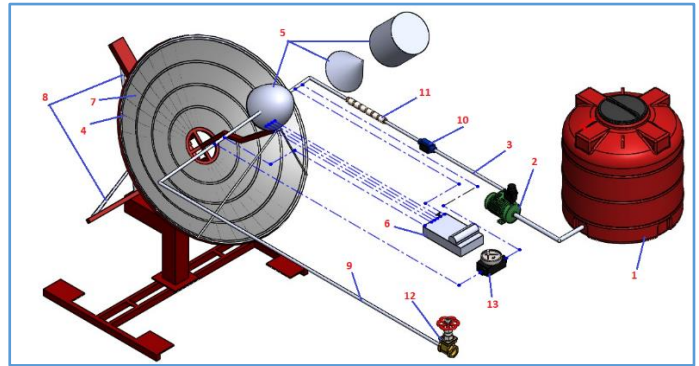**Fig. 1.** Photograph of the examined solar dish collector with a cavity receiver

Fig. 2. Elaborate scheme of the empirical system: 1. reservoir of the water, 2. pump, 3. tube for the inlet water, 4. rib, 5. Absorber (PDC_{cr}) models, 6. Temperatures measurement device, 7. reflective sheet, 8. Linear motors, 9. tube for the outlet water, 10. flowmeter, 11. heating source, 12. valve, 13. pressure drop measurement device

**Table 1.** Basic parameters of the experimental system

| Feature	Value	Feature	Value
Aperture area, A_a	3.04 m²	Material of the tubes	Copper
Concentrator outer diameter	2 m	Rim angle, ψ_r	45.24
Concentrator inner diameter	0.36 m	Working fluid	Water
Collector depth, C_d	208 mm	Concentration ratio, C_o	38
Focal length, f	1200 mm	Direct solar radiation, I_d	910.47

Fig. 3. Photograph of the heating source for the HTF inlet

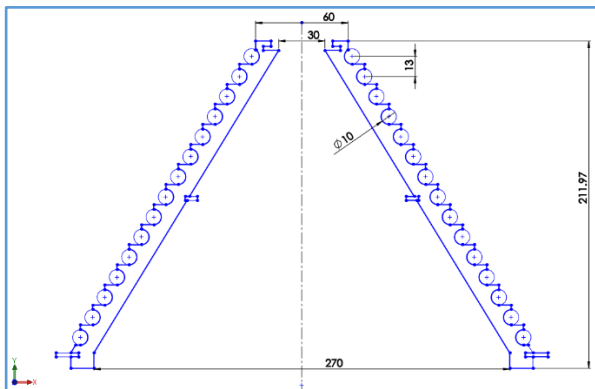## 3. Details of the PDC$_{cr}$ Models

In this study, three PDC$_{cr}$ samples were analyzed to estimate the receiver with the highest capability to transform solar energy. All receivers had a single flow path, and three design geometries, conical, oval, and cylindrical shapes, were investigated, as shown in Fig. 4.
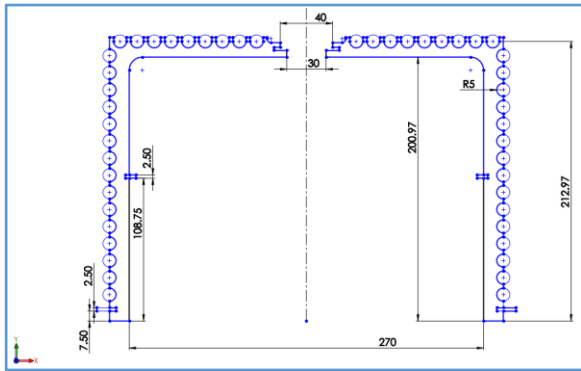
PDC$_{cr}$(1)
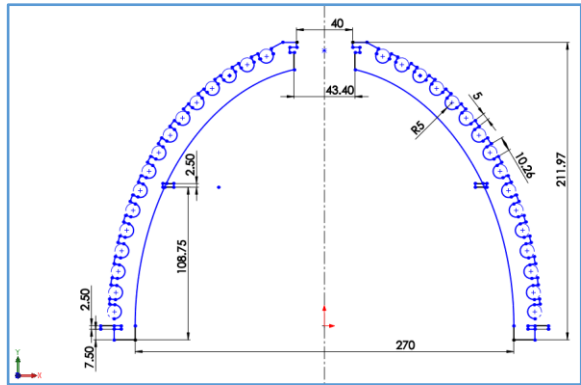
PDC$_{cr}$(2)

PDC$_{cr}$(3)

Fig. 4. Detailed views of the three PDC$_{cr}$ models

1; cylindrical, 2; oval, and 3; conical cavity receivers

All models were based on a copper structure manufactured by cutting a 3 mm copper plate with a water jet cutting machine and then assembling it into the three geometric shapes of solar collector, as shown in Fig. 5.
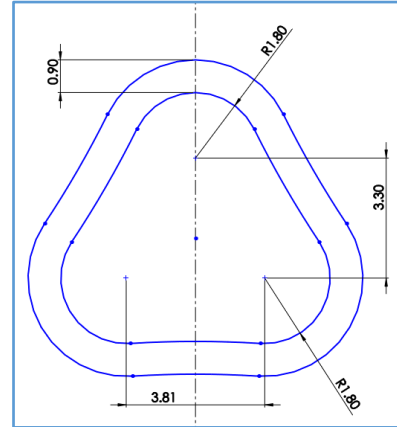

Fig. 5. Photographs of the copper structures of the three PDC$_{cr}$ models

Then, the tube was wrapped around the copper structure to form the final solar receiver, as shown in Fig. 6.

L_p = 28mm

Fig. 7. Detailed view of the cross section of the twisted tube that is used as the main pipe in the PDC_{cr}

Furthermore, the PDC_{cr} models were covered with a high-quality thermal insulation Teflon sheet with a thickness of 3 mm, as shown in Fig. 8.

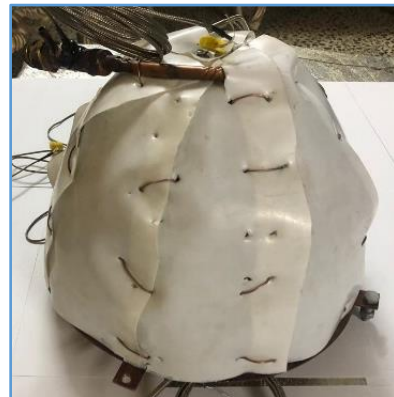**Fig. 6.** Photographs of the PDC_{cr} models after the copper structure was wrapped with the twisted tube

The main tube that is used to form the solar receiver is called the twisted tube, which is clarified in Fig. 7. It has the property of rotating the fluid during the flow in the pipe itself, which helps diffuse the heat energy absorbed by the fluid molecules running through the tube.

Fig. 8. Photographs of the PDC$_{cr}$ models after being covered with a high-quality thermal insulation Teflon sheet

Finally, the PDC$_{cr}$ models were joined with the dish collector, as shown in Fig. 9.

Fig. 9. Photographs of the PDC$_{cr}$ models after being placed in the focal center of the dish collector

4. Experimentation and Data Collection

The experimental tests were carried out at the University of Al Nahrain, College of Engineering (Latitude: 33°.27'N; longitude: 44°.38'E, Al-Jadriya, Baghdad). The experimental period occurred from August 1-20, 2019. During this period, measurements of the weather described sunshine, with an average maximum atmospheric temperature of 40.95℃, an average relative humidity of 17.31%, and an average wind speed of 1.96 m/s. The temperatures were recorded continuously every 30 seconds by the data logger. Additionally, the pressure drop through the receivers was recorded. The measurement process began when the PDC$_{cr}$ model was placed. Thereafter, five inlet temperatures of the HTF (12, 14, 16, 18, and 20℃) and three various values of ṁ (3, 6, and 9 L/min) were used to study the thermal performance of the different PDC$_{cr}$ models. When changing the inlet temperature, the flow rate was fixed at 3 L/min, and when changing the flow rate of the HTF, the inlet temperature was fixed at 12℃.

5. Mathematical Presentation

The mathematical details of this research have been analyzed minutely in Refs. [5, 17, 18]. In this research, only the main mathematical relations for the PDC$_{cr}$ are clarified.

5.1 Definitions of the performance

The available solar irradiation can be determined as follows:

$$Q_s = I_d A_a \tag{1}$$

The useful heat transfer rate Q_u between the PDC$_{cr}$ and the HTF is estimated by:

$$Q_u = \dot{m} C_p (T_{out} - T_{in}) \tag{2}$$

The thermal efficiency η_{th} of the SDC is the ratio of Q_u to Q_s:

$$\eta_{th} = Q_u / Q_s \tag{3}$$

Exergetic (or second law) estimation of the solar receiver is valuable in view of the fact that shows the quality of the operation. The thermal performance, operating temperatures, and pressure drop in the pipe are determined in the exergetic investigation. The useful exergy output rate is obtained by subtracting the irreversibility rate of the heating process from the exergy heat transfer rate, which can be determined as [5, 19]:

$$E_u = Q_u - \dot{m} \cdot C_p \cdot T_{am} \cdot ln(T_{out} / T_{in}) - \dot{m} \cdot T_{am} (\Delta P / \rho_{fm} \cdot T_{fm}) \tag{4}$$

The exergy rate of solar irradiation can be determined as [20]:

$$E_s = Q_s \cdot [1 - (4/3) \cdot (T_{am} / T_{sun}) + (1/3) \cdot (T_{am} / T_{sun})^4] \tag{5}$$

T_{sun} can be determined as 5770 K.

The exergetic performance of the PDC$_{cr}$ is estimated by the ratio of the useful exergy output to the solar exergy input [5, 19]:

$$\eta_{ex} = E_u / E_s \tag{6}$$

5.2 Heat transfer

As clarified in Ananth and Jaisankar [1, 21], Q_u can also be determined from:

$$Q_u = U_{wo} A_{wo} (T_{wo} - T_m) \qquad (7)$$

In addition,

$$(1/U_{wo} A_{wo}) = (1/h_{wi} A_{wi}) + (ln (D_{wo} / D_{wi}) / (2\pi K_w l)) \qquad (8)$$

Equation (8) can be written as:

$$h_{wi} = [(1/(U_{wo} A_{wo}) - ln (D_{wo} / D_{wi}) / (2\pi k_w l)) \times A_{wi}]^{-1}$$

By joining Eqs. (2), (7), and (8), the empirical Nu is obtained from:

$$N_u = h_{wi} D_{wi} / k_{HTF} \qquad (9)$$

All of the fluid thermophysical properties were estimated at the bulk mean temperature (T_m).

6. Results and Discussion

This study experimentally analyzed the thermal performance of three different shapes of PDC_{cr}, which consist of cylindrical, oval, and conical cavity receivers. Furthermore, the study takes into account the influence of changes in the input temperature of the HTF (with a range of 12-20 ℃) when $\dot{m}$=0.05 and the influence of changes in the mass flow rate of the HTF (with a range of 0.05-0.15 kg/s) when $T_i = 12℃$ on the performance of the receivers.

The outcomes of the experimental analysis present an enhancement of the temperature variance $\Delta T = T_{out} - T_{in}$, η_{th}, η_{ex}, Nu and the pressure difference for the conical cavity receivers.

Furthermore, the empirical uncertainties in the data lowering operation were estimated with indication to [22]. The greatest uncertainties of the five parameters indicate to previously were more or less ± 2.73%, ± 3.35%, ± 2.38%, ± 2.87%, and ± 3.41%, respectively.
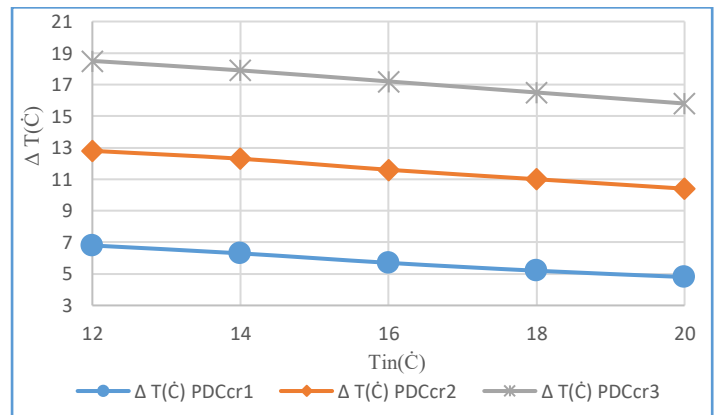
6.1 Temperature variance

As shown in Fig. 10 and Fig. 11, the highest values of the temperature difference $\Delta T(℃)$ were recorded for the conical cavity receivers, and the lowest values were recorded for the cylindrical cavity receivers; that is, the conical cavity model has the highest capability to transform incident energy on the receiver to thermal energy within HTF.

Furthermore, the results clarified that $\Delta T(℃)$ reduced with rising values of $\dot{m}$ of HTF for all PDC_{cr} shapes, as shown in Fig. 10, and smoothly decreases with increasing input temperature of the HTF for all PDC_{cr} models, as shown in Fig. 11, and the maximum $\Delta T(℃)$ is equal to 18.5℃ when $T_{in} = 12℃$ and $\dot{m} = 0.05$ kg/s.
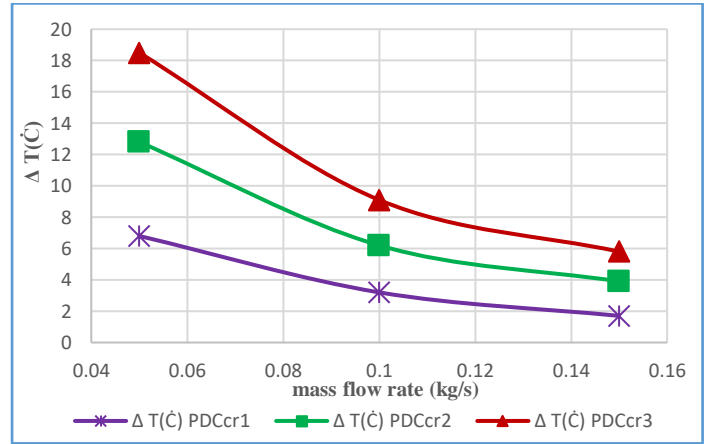
Fig. 10. Relationship between $\dot{m}$ and $\Delta T(℃)$ for all PDC_{cr} shapes (1; cylindrical, 2; oval, and 3; conical cavity receivers).
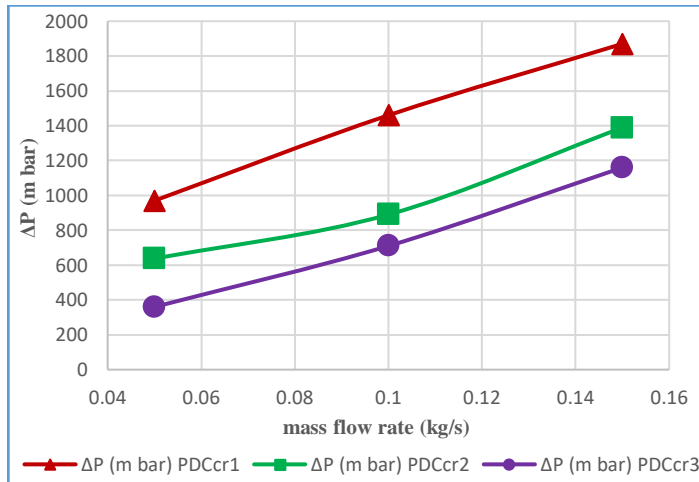

Fig. 11. Relationship between $T_{in}(℃)$ and $\Delta T(℃)$ for all PDC_{cr} shapes (1; cylindrical, 2; oval, and 3; conical cavity receivers).

6.2 Pressure difference

As shown in Fig. 12, the highest values of the pressure difference between the inlet and outlet of HTF through the receiver $\Delta p(m\ bar)$ were recorded for the cylindrical cavity receivers, and the lowest values were recorded for the conical cavity receivers; that is, the conical cavity model has the lowest pressure losses because the receiver has less length than the other receivers.

Additionally, $\Delta p(m\ bar)$ rises with rising $\dot{m}$ of the HTF for all PDC_{cr} shapes, as shown in Fig. 12, as a result of increased losses due to increasing mass flow rate.
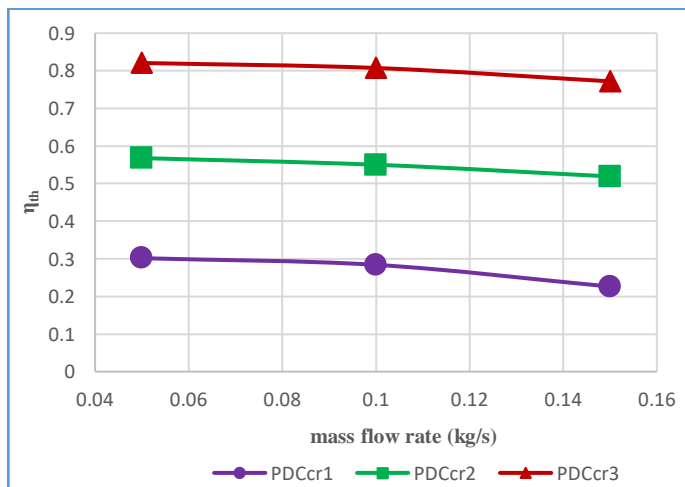
Fig. 12. Relationship between $\dot{m}$ and Δp for all PDC_{cr} shapes (1; cylindrical, 2; oval, and 3; conical cavity receivers).

6.3 Thermal efficiency, η_{th}

Based on Eq. (3), η_{th} was determined for each PDC_{cr} shape and various values of T_{in} and various values of $\dot{m}$ of the HTF. For all results, the highest values of η_{th} were recorded for the conical cavity receivers, and the lowest values were recorded for the cylindrical cavity receivers.

Furthermore, the results indicate that η_{th} reduced with rising values of $\dot{m}$ of HTF for all PDC_{cr} shapes, as shown in Fig. 13, and with rising input temperature of the HTF for all PDC_{cr} models, as shown in Fig. 14, and the maximum η_{th} is equal to 82.1% when $T_{in}=12\,°C$ and $\dot{m}=0.05$ kg/s.
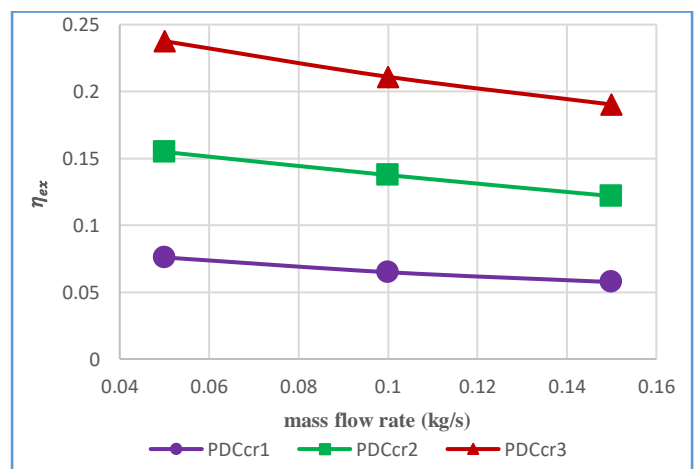

Fig. 13. Relationship between $\dot{m}$ and η_{th} for all PDC_{cr} shapes (1; cylindrical, 2; oval, and 3; conical cavity receivers).
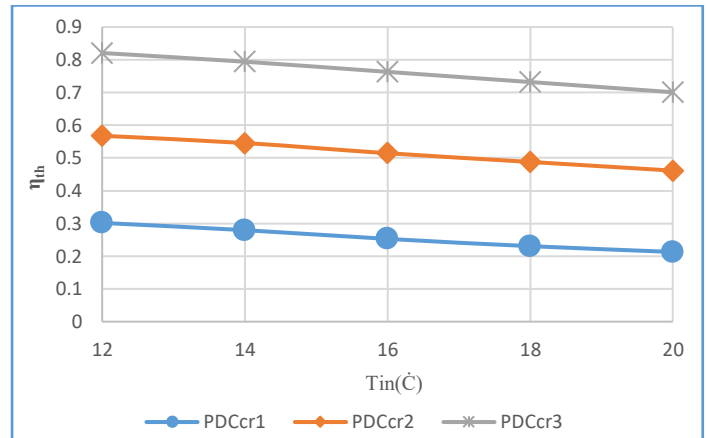
Fig. 14. Relevance between $T_{in}(°C)$ and η_{th} for all PDC_{cr} shapes (1; cylindrical, 2; oval, and 3; conical cavity receivers).

6.4 Exergetic performance, η_{ex}

The exergy efficiency η_{ex} takes into account the pumping work request and valuable heat production. Based on Eq. (6), η_{ex} was estimated for each PDC_{cr} model for different mass flow rates when $T_{in}=12°C$. The conical cavity receiver recorded the highest values of η_{ex}, as shown in Fig. 15. This is because the conical cavity receiver has the highest heat production and lowest pumping work. The maximum η_{ex} is equal to 23.76% when $T_{in}=12°C$ and $\dot{m}=0.05$ kg/s.

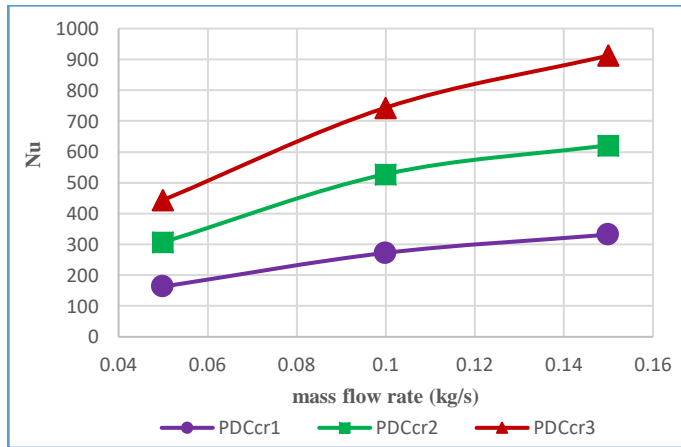**Fig. 15.** Relationship between $\dot{m}$ and η_{ex} for all PDC_{cr} shapes (1; cylindrical, 2; oval, and 3; conical cavity receivers).

6.5 Nusselt number Nu

As shown in Fig. 16 and Fig. 17, which refer to Nu with various values of T_{in} and various values of $\dot{m}$ of the HTF, which are calculated from Eq. (9), the results recorded the highest value of Nu for the conical cavity receiver.

As a result of the larger heat transfer rates, the model has the highest capability to absorb solar energy, which results in a rise in the $\Delta T(°C)$. This in turn augments the convective heat transfer to the inner side of the receiver tube.

Furthermore, the results indicate that Nu rises with rising values of $\dot{m}$ of HTF for all PDC$_{cr}$ shapes, as shown in Fig. 16, and smoothly decreases with rising T_{in} of the HTF for all PDC$_{cr}$ shapes, as shown in Fig. 17, and the maximum Nu is equal to 912.52 when T_{in} =12°C and $\dot{m}$=0.15 kg/s.

Fig. 16. Relationship between $\dot{m}$ and Nu for all PDC$_{cr}$ shapes (1; cylindrical, 2; oval, and 3; conical cavity receivers).
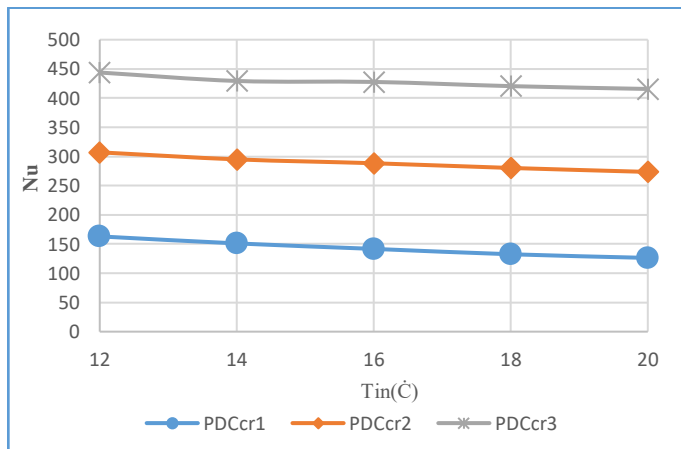
Fig. 17. Relationship between T$_{in}$(°C) and Nu for all PDC$_{cr}$ shapes (1; cylindrical, 2; oval, and 3; conical cavity receivers).

7. Conclusion

An experimental analysis was implemented to examine three geometries of PDC$_{cr}$ for transform incident energy on the receivers to thermal energy within HTF. Models including cylindrical, oval, and conical cavity receivers were analyzed and tested to estimate the optimum geometry for dish collector cavity receivers PDC$_{cr}$. The analysis was carried out by estimating ΔT, ΔP, η_{th}, η_{ex}, Nu for various values of $\dot{m}$ (3, 6, and 9 L/min) and various values of inlet temperatures of the HTF (12, 14, 16, 18, and 20 °C). The results of the investigations showed that the conical cavity receiver owns the greatest value of thermal performance compared with the other shapes of receivers, with values of η_{th}=82.1%, η_{ex}=23.76%, and Nu=912.52.

Nomenclature

Symbols

A	Area [m^2]
$C_o = A_a / A_r$	Concentration ratio [-]
Cd	Collector depth [m]
c_p	Specific heat capacity, estimated to be a function of the average temperature of the PDC$_{cr}$ [J/kg/K]
D	Diameter [m]
E	Exergy flow rate [W]
f	Focal length [m]
I_d	Direct solar radiation [W/m^2]
Q	Heat transfer rate [kW]
$\dot{m}$	Mass flow rate of water HTF [kg/s]
T	Temperature [°C]
Δp	Pressure drop [**m bar**]
U	Overall heat transfer coefficient (W/m^{2}k)
h	Average convective heat transfer coefficient (W/m^2°C)
l	Length (m)
k	Thermal conductivity (W/m°C)

Greek letters

ψ	Rim angle [°]
η	Efficiency [-]
ρ	Density [kg/m^3]

Abbreviations

PDC$_{cr}$	parabolic dish collector cavity receivers
PDC	parabolic dish collector
HTF	Heat transfer fluid
MCRT	Monte Carlo ray-tracing
FVM	Finite volume method

Subscripts and superscripts

a	aperture
am	ambient
ex	exergetic
fm	mean fluid, bulk mean temperature of the fluid in PDC$_{cr}$ ((T$_{in}$+T$_{out}$)/2)[°C]
in	inlet
out	outlet
s	solar

sun	Sun
th	thermal
u	useful
wo	Outside surface of the tube of the receiver
wi	Inside surface of the tube of the receiver

References

[1] R. K. M. Aldulaimi. (2019). "An Innovative Receiver Design for a Parabolic Trough Solar Collector Using Overlapped and Reverse Flow: An Experimental Study", Arabian Journal for Science and Engineering, vol. 44, pp. 7529–7539.

[2] M. S. Söylemez, R. K. M. Aldulaimi. (2016). "An innovative optimization algorithm for precis estimation of the optical efficiency of heliostat fields", International journal of renewable energy research, vol. 6, pp. 759-771.

[3] W. Fuqiang, C. Ziming, T. Jianyu, Y. Yuan, S. Yong, L. Linhua, (2017), "Progress in concentrated solar power technology with parabolic trough collector system: a comprehensive review", Renew Sustain Energy Rev, vol. 79, pp. 1314–28.

[4] P. Sasa, B. Evangelos, G. Willem Le Roux, S. Velimir, T. Christos, (2017). "Experimental investigation and parametric analysis of a solar thermal dish collector with spiral absorber", Applied Thermal Engineering, vol. 121, pp. 126-135.

[5] R. K. M. Aldulaimi, (2020), "Experimental investigation of the receiver of a solar thermal dish collector with a dual layer, staggered tube arrangement, and multiscale diameter", Energy Exploration & Exploitation.

[6] V. Thirunavukkarasu, M. Cheralathan, (2020), "An experimental study on energy and exergy performance of a spiral tube receiver for solar parabolic dish concentrator", Energy, vol. 192.

[7] X. Lan, G. Feng-Wei, W. Shuang-Ying, C. Zhi-Li, (2020), "A comprehensive simulation on optical and thermal performance of a cylindrical cavity receiver in a parabolic dish collector system", Renewable Energy, vol. 145, pp. 878-892.

[8] L. Reyhaneh, E. Askari Asli-Areh, B. Ghobadian, A. B. Kasaeian, Sh. Gorjian, G. Najafi, B. Evangelos, (2020). "Research and review study of solar dish concentrators with different nanofluids and different shapes of cavity receiver: Experimental tests", Renewable Energy, vol. 145, pp. 783-804.

[9] A. Kuldeep, K. K. Mohd , (2019), "Performance evaluation of coiled tube receiver cavity for a concentrating collector", Renewable Energy, vol. 138, pp. 666-674.

[10] R. Alireza, A. Ali Sulaiman, M. Shuhaimi, L. Reyhaneh, N. Gholamhassan, K. Alibakhsh, (2019), "Thermal analysis of a hybrid solar desalination system using various shapes of cavity receiver: Cubical, cylindrical, and hemispherical". Energy Conversion and Management, vol. 198, pp. 111861

[11] L. Ovidio, B. Alfonso, A. Aurelio, (2019), "On the thermal performance of flat and cavity receivers for a parabolic dish concentrator and low/medium temperatures", Solar Energy.

[12] B. Evangelos, B. Erion, T. Christos, P. Sasa, (2019), "Optical and thermal analysis of different cavity receiver designs for solar dish concentrators", Energy Conversion and Management, vol. 2.

[13] S. Sara, B. Mohammad, A. Vahid Madadi, (2019), "A novel optical-thermal modeling of a parabolic dish collector with a helically baffled cylindrical cavity receiver", Energy, vol. 168, pp. 88-98.

[14] R. Loni, A.B. Kasaeian, E. Askari Asli-Ardeh, B. Ghobadian, Sh. Gorjian, (2018), "Experimental and Numerical Study on Dish Concentrator with Cubical and Cylindrical Cavity Receivers using Thermal Oil", Energy, vol. 154, pp. 168-181.

[15] M. Daabo Ahmed, M. Saad, R. K. Al-Dadah, (2016), "The effect of receiver geometry on the optical performance of a small scale solar cavity receiver for parabolic dish applications", Energy, vol. 114, pp. 513-525.

[16] B. Evangelos, T. Christos, (2019), "A review of concentrating solar thermal collectors with and without nanofluids", Journal of Thermal Analysis and Calorimetry, vol. 135, pp. 763-786.

[17] R. Loni, S. Pavlovic, E. Bellos, C. Tzivanidis, E.A. Asli-Ardeh, (2018), "Thermal and exergy performance of a nanofluid-based solar dish collector with spiral cavity receiver", Applied Thermal Engineering, vol. 135, pp. 206-217.

[18] P. Stefanovic Velimir, R. Pavlovic Sasa, B. Evangelos, T. Christos, (2018), "A detailed parametric analysis of a solar dish collector", Sustainable Energy Technologies and Assessments, vol. 25, pp. 99–110.

[19] E. Bellos, C. Tzivanidis, K.A. Antonopoulos. (2017). "A detailed working fluid investigation for solar parabolic trough collectors", Applied Thermal Engineering, vol. 114, pp. 374-386.

[20] P. Richard, (2003). "Exergy of undiluted thermal radiation". Solar Energy, vol. 74, pp. 469–488.

[21] J. Ananth, S. Jaisankar, (2013), "Experimental studies on heat transfer and friction factor characteristics of thermosyphon solar water heating system fitted with regularly spaced twisted tape with rod and spacer", Energy Convers. Manag., vol. 73, pp. 207–213.

[22] H. W. Coleman, W. G. Steele, Experimental and Uncertainty Analysis for Engineers, Wiley Interscience, New York (1989).